Semiconductor Science and Technology

ACCEPTED MANUSCRIPT

Heteroepitaxial β-Ga_2O_3 thick films on sapphire substrate by carbothermal reduction rapid growth method

To cite this article before publication: Wenhui Zhang *et al* 2022 *Semicond. Sci. Technol.* in press https://doi.org/10.1088/1361-6641/ac79c7

Manuscript version: Accepted Manuscript

Accepted Manuscript is “the version of the article accepted for publication including all changes made as a result of the peer review process, and which may also include the addition to the article by IOP Publishing of a header, an article ID, a cover sheet and/or an ‘Accepted Manuscript’ watermark, but excluding any other editing, typesetting or other changes made by IOP Publishing and/or its licensors”

This Accepted Manuscript is **© 2022 IOP Publishing Ltd**.

During the embargo period (the 12 month period from the publication of the Version of Record of this article), the Accepted Manuscript is fully protected by copyright and cannot be reused or reposted elsewhere.
As the Version of Record of this article is going to be / has been published on a subscription basis, this Accepted Manuscript is available for reuse under a CC BY-NC-ND 3.0 licence after the 12 month embargo period.

After the embargo period, everyone is permitted to use copy and redistribute this article for non-commercial purposes only, provided that they adhere to all the terms of the licence https://creativecommons.org/licences/by-nc-nd/3.0

Although reasonable endeavours have been taken to obtain all necessary permissions from third parties to include their copyrighted content within this article, their full citation and copyright line may not be present in this Accepted Manuscript version. Before using any content from this article, please refer to the Version of Record on IOPscience once published for full citation and copyright details, as permissions will likely be required. All third party content is fully copyright protected, unless specifically stated otherwise in the figure caption in the Version of Record.

View the article online for updates and enhancements.

This content was downloaded from IP address 202.118.73.139 on 22/06/2022 at 04:09

IOP Publishing Semiconductor Science and Technology
Journal **XX** (XXXX) XXXXXX https://doi.org/XXXX/XXXX

Heteroepitaxial β-Ga_2O_3 thick films on sapphire substrate by carbothermal reduction rapid growth method

Wenhui. Zhang[1], Hezhi. Zhang[1,2,a)], Zhenzhong. Zhang[1], Qi. Zhang[2], Xibing. Hu[2] and Hongwei. Liang [1,a)]

[1] School of Microeletronics, Dalian University of Technology, Dalian, 116024, People's Republic of China
[2] Jiangsu Xinguanglian Technology Company Ltd., Wuxi, 214192, People's Republic of China

a) E-mail: hez.zhang@dlut.edu.cn and hwliang@dlut.edu.cn

Received xxxxxx
Accepted for publication xxxxxx
Published xxxxxx

Abstract

The heteroepitaxial β-Ga_2O_3 thick films were rapidly grown on various oriented sapphire substrates using carbothermal reduction method. The β-Ga_2O_3 films were prepared in our home-made vertical dual temperature zone furnace. The growth direction as well as surface morphology showed the strong dependence on the orientation of the sapphire substrate. The fastest growth rate was obtained reaching approximate 15 μm/h on c-plane sapphire substrate according to the average 30 μm thickness of β-Ga_2O_3 films grown for 2 hr measured by cross-section scanning electron microscope. The Raman spectra indicated the pure-phase β-Ga_2O_3 films without obvious strain. The bandgap for grown films were in range of 4.6-4.7 eV confirmed by X-ray photoelectron spectra and Tauc plot from absorption spectra. Secondary ion mass spectrometry was used to check the impurities indicating a limited amount of residual carbon inside the films even though graphite as the reducing agent. The results in this work give promising alternative method of rapid epitaxial β-Ga_2O_3 thick films for the application on high-power electronic devices.

Keywords: β-Ga_2O_3 thick films, carbothermal reduction method, rapid growth

1. Introduction

Thermodynamically stable β-gallium oxide (Ga_2O_3) is one of the promising ultrawide bandgap semiconductor material attribute to the large bandgap (4.8 eV), high breakdown electrical field and Baliga's figure of merit [1]. Moreover, high quality β-Ga_2O_3 bulk synthesized by simple and low-cost melt growth methods [2, 3] have been successfully prepared for large scale substrate which is well-suited for commercial using. By these superior advantages, various devices based β-Ga_2O_3 have been reported such as photodetectors, high power electronics and radiation hard devices [4-8].

In the application of Schottky barrier diodes based on β-Ga_2O_3, epitaxial high-purity β-Ga_2O_3 thick films with low carrier density enable to exploit the intrinsic advantage to achieve higher breakdown voltage and lower on-resistance [9,10]. For the state of art β-Ga_2O_3 based Schottky barrier diodes, the drift region is usually above 10 μm [11,12]. Such thickness require the relative fast growth rate. At present, synthesizing β-Ga_2O_3 films have been extensively studied by pulsed laser deposition (PLD) [13], molecular beam epitaxy (MBE) [14], plasma-enhanced chemical vapor depostion (PECVD) [15], metal organic vapor deposition (MOCVD) [16], low pressure chemical vapor deposition (LPCVD) [17], halide vapor phase epitaxy (HVPE) [18,19] and etc. Among them, PLD and MBE are not suitable on growth of thick β-Ga_2O_3 films due to the low growth rate (<1 μm/h). PECVD, LPCVD and MOCVD exhibited moderate growth rate (1~2 μm/h) are alternative methods, nevertheless, the growth rate is still not sufficient enough for sythersizing thick films. At present, HVPE exhibited the advantage of fast growth rate (>5 μm/h), reasonable quality and controllable doping quantity are the most popular approach. The homoexpitaxial and heteroexpitaxial on sapphire substrate by HVPE have been reported widely. Murakami*et al.* [18,20] firstly reported that homoepitaxial high-purity β-Ga_2O_3 thick films with growth rate of 5 μm/h grown on (001) β-Ga_2O_3 substrate by HVPE, and fabricated MESFET and SBD devices based on β-Ga_2O_3 thick films. Nikolaev *et al* [21] reported that the fastest growth rate of β-Ga_2O_3 films prepared by HVPE up to now reaching 250 μm/h. Li *et al* [19] reported that the (-201) β-Ga_2O_3 films with growth rate of 4 μm/h grown on c-plane sappphire substrate by HVPE, as well as investigated the microstructure properties of heteroepitaxial β-Ga_2O_3 films. Neverthelss, the growth process of HVPE invovled corrosive precussors such as HCl and Cl_2 gas result in the substrate etching and creating the unavoidable defect [22], which further limit to improve the film quality. Therefore, it is neccesary to develop the alternative growth method without corrosive precussors gas.

Carbothermal reduction was a widely reported method on sythesizing β-Ga_2O_3 nanostructure [23, 24], neverthless, the β-Ga_2O_3 films has never been realized. The advantages of carbothermal reduction is the use of non-corrosive materials (Ga_2O_3 and grahite powder). The reaction mechnism of carbothermal reduction process contain two stages: (I) Ga_2O_3 powder is significant decomposed into Ga_2O and CO by reductant of graphite power over 1000℃. (II) the suboxide Ga_2O vapor continuously react with CO to produce Ga and CO_2. In the aspect of nanostructrure growth, the growth condition under the atmosphere of Argon (Ar) providing a metal-rich condition is helpful for Ga droplets gathered on substrate leading to the self-catalyzed nanostructure growth. Whereas, according to the theoretical analyse, maintaining large amount of Ga_2O vapor and the Ga_2O vapor reoxided with O_2 is the key for fast growth of Ga_2O_3 thick films [25, 26]. Therefore, it is strongly recommended to promote the first stage of the carbothermal reduction and inhibit the second stage. In this paper, we demonstrated fast expitaxial β-Ga_2O_3 thick films by carbothermal reduction method. The growth was taken place in our home-made vertical dual temperature furnace under certain growth condition. The raw material was placed at the lower part of furnace setting at 1400℃ for generating sufficient Ga_2O vapor. The substrate was placed in oxygen rich enviroment in the upper of furnace setting at 950℃, meanwhile keeping an oxygen rich enviroment by 100sccm O_2 flow, which can prevent Ga_2O vapor decompostion and allow reoxided Ga_2O vapor to form β-Ga_2O_3 layers. The growth rate was examined to be 15 μm/h, 10 μm/h, and 4 μm/h, respectively, for c-plane (0001), m-plane (10-10), and r-plane (1-102) sapphire substrate. The material properties of as grown films were characterized in detail. The SIMS results indicate the limited carbon residual inside the thick films although the graphite power was introduced as the reducing agent.

2. Experiments

The growth of β-Ga_2O_3 thick films was proceed in a home-made vertical dual temperature zone furnace, as illustrated in figure 1. High purity Ga_2O_3 powder (99.999%) mixed with graphite powder (molar ratio of 1:20) as the source material was put in the corundum crucible where placed at the lower part of the furnace. The sapphire substrate was placed at the upper part of the furnace. The setting temperature was at 1400 ℃ and 950 ℃, for lower and upper part of furnace, respectively. The growth process was taken place under the oxygen-rich enviroment maintaining by 100 sccm Oxygen (O_2) and 500 sccm Argon (Ar) for 2 hr at pressure of 3×10^3 Pa. Through the reduction of graphite powder, Ga_2O_3 powder is decomposed into Ga_2O (g) and O_2 at high temperature region shown as follow:

$$Ga_2O_3\,(s) + 2C\,(s) \rightarrow Ga_2O\,(g) + 2CO\,(g) \qquad (1)$$

Ga_2O vapor was transported to substrate surface and then re-react O_2 at low temperature region to form β-Ga_2O_3 films as represented below:

$$Ga_2O\,(g) + O_2\,(g) \rightarrow Ga_2O_3\,(s) \qquad (2)$$

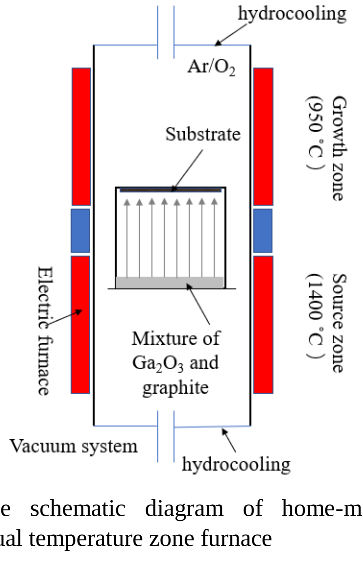

FIG. 1. The schematic diagram of home-made vertical cylindrical dual temperature zone furnace

3. Results and discussions

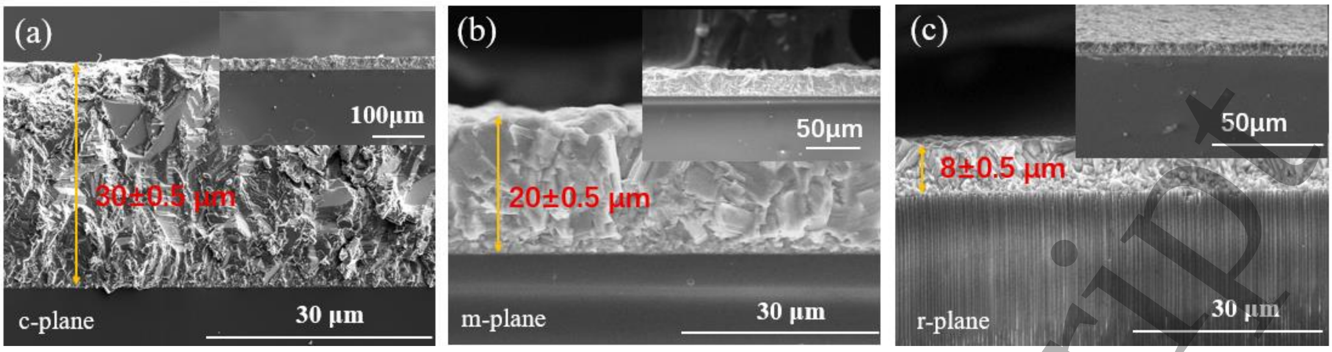

FIG. 2. The cross-section SEM images of β-Ga_2O_3 films grown on (a) c-plane (0001), (b) m-plane (10-10) and (c) r-plane (1-102) sapphire substrates, respectively.

The growth rate for β-Ga_2O_3 thick films were characterized by cross-section scanning electron microscopy (SEM, FEI Nova Nano 450) images as shown in figure 2. Insets of figure 2 depict the cross-section image in low magnification which present the films uniformity as well as a clear interface. The growth rate was estimated to be 15, 10 and 4 μm/h according to the average thickness of 30, 20 and 8 μm, respectively, for grown on c-plane, m-plane and r-plane sapphire substrates. According to the theoretical calculation [15, 27], the lattice mismatch rate of short and long side between (-201) plane of β-Ga_2O_3 and c-plane sapphire, (100) plane of β-Ga_2O_3 and m-plane sapphire, (100) plane of β-Ga_2O_3 and r-plane sapphire, are 4.87% and 4.5%, 17% and 12%, 35.5% and 32.7%, respectively. The different mismatch related strain results in the different atom binding energy which means the different nucleation as well as the growth rate can be observed. This could be the explanation that (-201) plane of β-Ga_2O_3 on c-plane sapphire substrate has the fastest growth rate whereas (100) plane of β-Ga_2O_3 on r-plane sapphire substrate has the lowest growth rate. The rapid growth achieved by

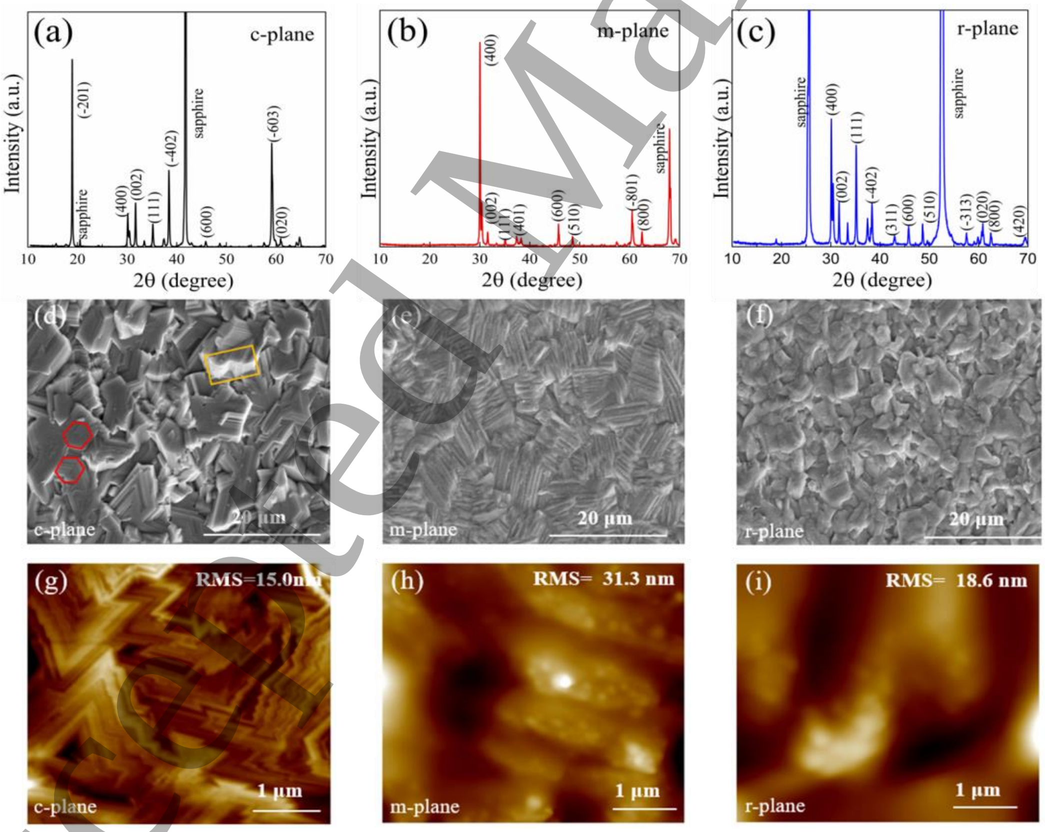

FIG. 3. XRD results of β-Ga_2O_3 films grown on (a) c-plane (0001), (b) m-plane (10-10), and (c) r-plane (1-102) sapphire substrates. The corresponding surface SEM results shown in image (d), (e) and (f), respectively. The corresponding AFM results shown in image (g), (h) and (i), respectively.

carbothermal reduction could be an alternative method to growth β-Ga_2O_3 thick films to satisfy the demand for the β-Ga_2O_3 devices with thick drift region [11,12,18,20].

To determine the crystalline orientation, surface morphology and roughness on different sapphire substrates, the as-grown Ga_2O_3 thick films were investigated by X-ray diffraction (XRD, Bruker D8 Advance), top-view scanning electron microscopy (SEM, FEI Nova Nano 450) and atomic force microscopy (AFM, Bruker Dimension Icon). For the films grown on c-plane sapphire (Fig 3(a)), three main diffraction peaks are visible at 18.95, 38.43, and 59.13° referring to (-201) and high order planes of β-Ga_2O_3 grown parallel to the (0001) sapphire substrate, which is due to the approximate atomic arrangement (equilateral triangles) of oxygen atoms near the β-Ga_2O_3 (-201) plane and c-plane (0001) sapphire substrate [28]. In previous literature, the β-Ga_2O_3 films grown on c-plane (0001) sapphire substrate with (-201) preferred growth orientation had been widespread reported by MBE, MOCVD and PLD [16,28,30]. The strong (-201) orientation leads to the quasi six-fold rotational surface morphology noted in the red hexagonal area as shown in figure 3(d). The additional subpeak in XRD results index (400), (002) and (111) is attributed to the rhombic prism faces appearance as shown in the orange rectangular area since the lattice mismatch leading to the anisotropic growth happened. The AFM image in figure 3(g) is well correlated with SEM image showing the root mean square (RMS) roughness around 15.0 nm. The lattice mismatch between the c-plane sapphire substrate and β-Ga_2O_3 (-201) plane, which result in the 3D growth of columnar particles with poor crystalline symmetry for β-Ga_2O_3 films under the fast growth rate. The XRD result of the films grown on m-plane sapphire substrate (Fig 3(b)) shows the peak position suited at around 30.03, 45.77 and 62.49° in accordance with the (400), (600) and (800) diffraction peaks of β-Ga_2O_3, respectively. The [100] direction of β-Ga_2O_3 grown along m-plane sapphire substrate was confirmed by Nakagomi *et al* [31], which reported that twelve kinds of β-Ga_2O_3 crystal orientations including β-Ga_2O_3 (400) plane on m-plane sapphire using X-ray pole figure analyses. The top view SEM displays the surface morphology of large granular structure (average size ~10 μm) composed of azimuthal shape crystal in figure 3(e). Nevertheless, the RMS of film on m-plane sapphire (~31 nm shown in figure 3(h)) is much higher. The reason is probably due to the tetrahedral morphology at primary growth stage for β-Ga_2O_3 films grown on m-plane, which result in the regular oriented isometric crystals with the azimuthal shape under fast growth rate [15]. The films on r-plane sapphire substrate exhibits only granular with prismatic shape structure (Fig 3(f)) with 18.6 nm RMS surface roughness (Fig 3(i)), however, the XRD result shows the weak (400), (600) and (800) β-Ga_2O_3 diffraction peaks in figure 3(c). Considering the crystal orientation of between β-Ga_2O_3 films and the sapphire substrate surface, the oxygen atoms of m-plane and r-plane sapphire substrate have the similar rectangular arrangement as β-Ga_2O_3 (100) plane, which contribute to the appearance of (400), (600), and (800) peaks of β-Ga_2O_3 films on m-plane and r-plane sapphire substrates.

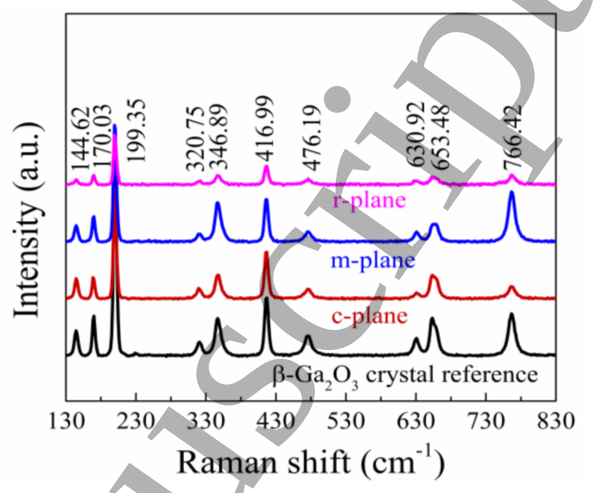

FIG. 4. The Raman spectra of β-Ga_2O_3 crystal reference and β-Ga_2O_3 films grown on c-plane (0001), m-plane (10-10), and r-plane (1-102) sapphire substrates.

Figure 4 depicts the Raman spectra (Renishaw InVia03) of β-Ga_2O_3 films grown on different sapphire substrates. A β-Ga_2O_3 single crystal is used as reference. β-Ga_2O_3 is the C_{2h} space group monoclinic structure composed of Ga_2O_6 octahedra and GaO_4 tetrahedra. The oscillation modes are categorized into low (from 140 cm^{-1} to 200 cm^{-1}), medium (from 320 cm^{-1} to 480 cm^{-1}) and high frequency (from 630 cm^{-1} to 730 cm^{-1}) mode representing the tetrahedra-octahedra chains vibration, the deformation of Ga_2O_6 octahedra, and the bending and stretching of the GaO_4 tetrahedron, respectively. Compared to the reference β-Ga_2O_3 single crystal, each peak

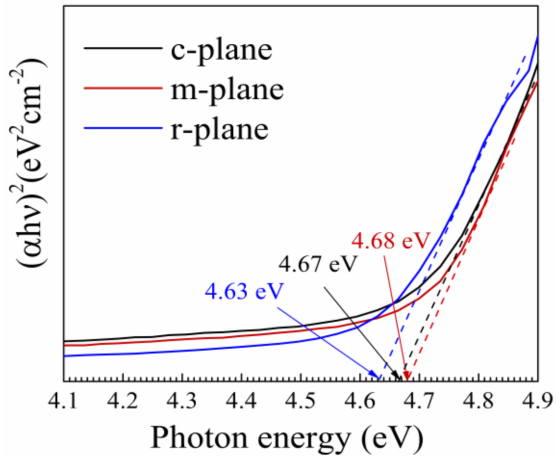

FIG. 5. The Tauc plot with $(\alpha h\nu)^2$ as a function of photo energy (hν) for β-Ga_2O_3 films grown on sapphire substrates of different orientations: c-plane (0001), m-plane (10-10), and r-plane (1-102).

position for epitaxial thick films on different sapphire substrate do not exhibit the apparent position shift indicating the obtained films are pure phase β-Ga_2O_3 with limited residual strain.

coincident with that of results estimated by Tauc plot in absorption spectra. The estimated bandgap value of β-Ga_2O_3 films grown on various sapphire substrates are in the range of 4.5-4.8 eV as previous report [15,32].

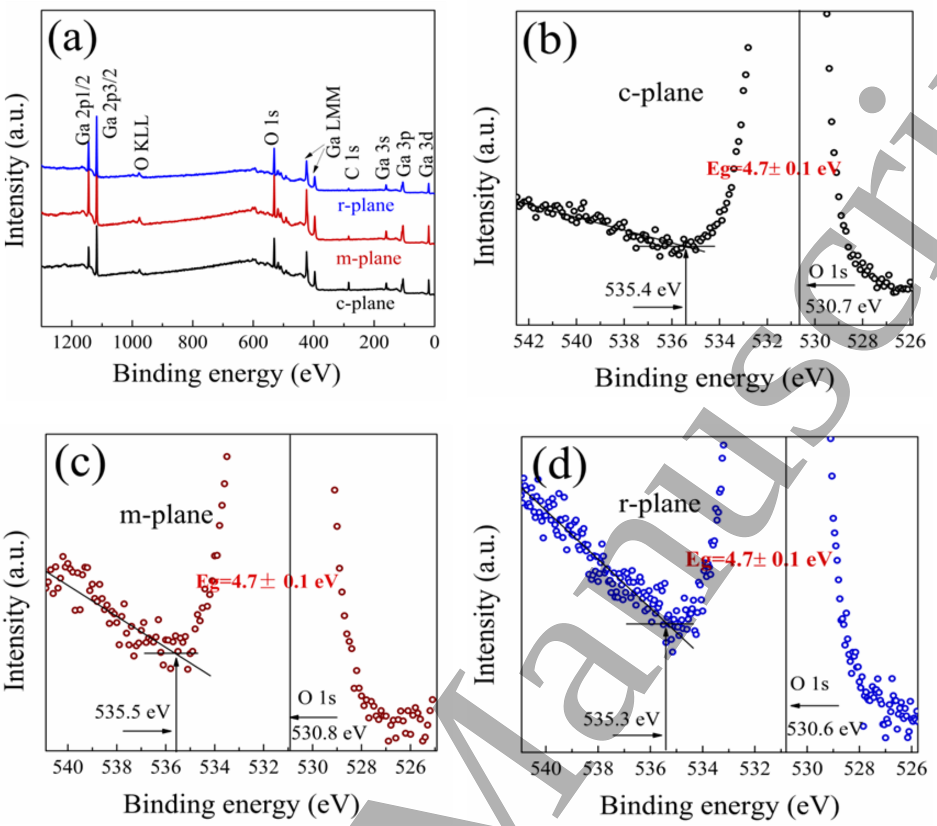

FIG. 6. (a) The XPS wide survey spectra of β-Ga_2O_3 films grown on c-plane (0001), m-plane (10-10), and r-plane (1-102) sapphire substrates. (b)-(d) The peak energy and the inelastic losses of O 1s for β-Ga_2O_3 films grown on c-plane (0001), m-plane (10-10), and r-plane (1-102) sapphire substrates.

The optical bandgap was estimated by the Tauc plot with $(\alpha h\nu)^2$ as a function of photon energy (hν) for β-Ga_2O_3 films grown on different sapphire substrates from absorption spectra measured by ultraviolet-visible spectrophotometer (Shimadzu UV3600) displayed in figure 5. According to formula $(\alpha h\nu)^2 = A(h\nu - E_g)$, where α is the absorption coefficient and hν is the energy of incident photon, the optical bandgap of β-Ga_2O_3 films is 4.67 eV, 4.68 eV, and 4.63 eV for grown on c-plane, m-plane, and r-plane sapphire substrates, respectively.

The bandgap of as grown β-Ga_2O_3 thick films is further approved by X-ray photoelectron spectroscopy (XPS, K-alpha+) measurement. Figure 6(a) shows The XPS wide survey spectra calibrated according to the peak position of Carbon 1s. The energy bandgap of β-Ga_2O_3 thick films is characterized by the difference value between the peak energy and the initial value of inelastic loss for O 1s. From figure 6(b) to figure 6(d), the bandgap extracted from the detailed O 1s spectra are all around 4.7 ± 0.1 eV for β-Ga_2O_3 films grown on c-plane, m-plane, and r-plane sapphire substrates, which is

Since the growth process involved the graphite as reducing agent, it is necessary to examine the impurities inside. Figure 7 shows time-of-flight secondary ion mass spectrometry

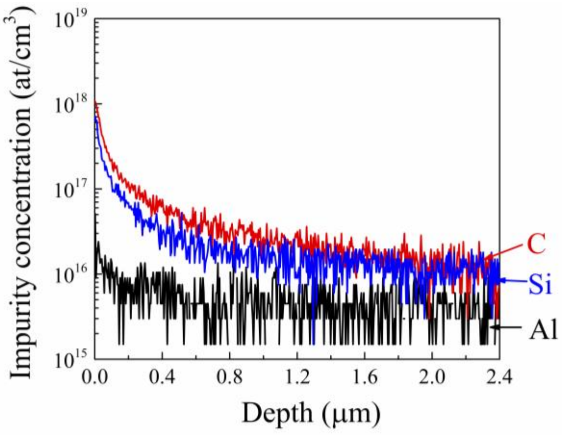

FIG. 7. The TOF-SIMS depth profile of β-Ga_2O_3 films grown on c-plane (0001) sapphire substrate.

(TOF-SIMS, IONTOF 5) element depth profiles for heteroepitaxial β-Ga_2O_3 films grown on c-plane sapphire substrate. The surface of β-Ga_2O_3 films contains a small amount of C and Si elements due to the enrichment effect of impurities on film surface [9]. As the deeper inside the films, the concentration of C and Si impurities is declined significantly closing to the detection limit (~10^{16} at/cm^3) as using aluminum (Al) as reference. The relative low number of C impurity in the films indicates the merely impact for Ga_2O_3 films epitaxial by carbothermal reduction in our experiment although the most effort for HVPE and MOCVD on controlling carbon involvement. Moreover, the room temperature Hall mobility and carrier concentration of β-Ga_2O_3 films grown on c-plane sapphire substrate were measured by Hall effect (Lake Shore 7704 A). The room temperature carrier concentration of β-Ga_2O_3 films grown by carbothermal reduction method is approximate 10^{15} cm^{-3} with Hall mobility of 22.5 cm^2/Vs as shown in Table 1, although the results are strongly affected by ohmic contact as well as the crystal quality. The further effort will be the homoepitaxy on semi-insulating Ga_2O_3 substrate to confirm the exact carrier concentration and Hall mobility.

Table 1. The room temperature carrier concentration and Hall mobility of β-Ga_2O_3 films using carbothermal reduction method

Method	Carrier concentration (cm^{-3})	Hall mobility (cm^2/Vs)
Carbothermal reduction	10^{15}	22.5

4. Conclusions

In this paper, we report that successfully grown β-Ga_2O_3 thick films by carbothermal reduction method on different sapphire substrates. The growth was prepared in a home-made vertical cylindrical dual temperature zone furnace with the source material of high purity Ga_2O_3 powder (99.999%) mixed with graphite powder (molar ratio of 1:20). The growth direction as well as surface morphology of as-grown β-Ga_2O_3 films are strongly dependent on the orientation of sapphire substrates. The β-Ga_2O_3 film grown on c-plane sapphire substrate exhibited a faster growth rate of 15 μm/h and lower surface roughness of 15.0 nm in comparison with films on r-plane and m-plane sapphire substrates. The Raman spectra indicated the pure-phase β-Ga_2O_3 films without obvious strain. The bandgap estimated from the O 1s spectra in XPS for β-Ga_2O_3 films grown on various oriented sapphire substrates is consistent with the optical bandgap using Tauc plot in absorption spectra, which in range of 4.6-4.7 eV. The SIMS results present relative low number of C and Si impurities in the films indicating the merely impact for Ga_2O_3 films by using graphite powder as reducing agent in our experiment. The room temperature low carrier concentration for ~10^{15} cm^{-3} and Hall mobility for 22.35 cm^2/Vs of obtained β-Ga_2O_3 films.

Data availability statement

The data that support the findings of this study are available from the corresponding author upon reasonable request.

Acknowledgment

This work was supported by the National Natural Science Foundation of China under Grant 62104024, Grant 11875097, Grant 12075045, Grant 11975257, Grant 11961141014, Grant 62074146; the Fundamental Research Funds for the Central Universities under Grant DUT19RC (3)074; the Natural Science Foundation of Liaoning Province under Grant 2021MS124, Grant 2020MS243 and the Ministry of Industry and Information Technology of the People's Republic of China

References

[1] H. Xue, Q. He, G. Jian, S. Long, T. Pang and M. Liu, *Nanoscale Res. Lett.* **13**, 290 (2018).

[2] M. Higashiwaki, K. Sasaki, A. Kuramata, T. Masui and S. Yamakoshi, *Appl. Phys. Lett.* **100**, 013504 (2012).

[3] K. Hoshikawa, E. Ohba, T. Kobayashi, J. Yanagisawa, C. Miyagawa and Y. Nakamura, *J. Cryst. Growth* **447**, 36-41 (2016).

[4] S. J. Pearton, F. Ren, M. Tadjer and J. Kim, *J. Appl. Phys.* **124**, 220901 (2018).

[5] S. Li, J. Yue, C. Lu, Z. Yan, Z. Liu, P. Li, D. Guo, Z. Wu, Y. Guo and W. Tang, *Sci. China Tech. Sci.* **65** (3), 704-712 (2022).

[6] G. Ma, W. Jiang, W. Sun, Z. Yan, B. Sun, S. Li, M. Zhang, X. Wang, A. Gao, J. Dai, Z. Liu, P. Li and W. Tang, *Phys. Scr.* **96**, 125823 (2021).

[5] S. Li, J. Yue, C. Lu, Z. Yan, Z. Liu, P. Li, D. Guo, Z. Wu, Y. Guo and W. Tang, *Sci. China Tech. Sci.* **65** (3), 704-712 (2022).

[6] G. Ma, W. Jiang, W. Sun, Z. Yan, B. Sun, S. Li, M. Zhang, X. Wang, A. Gao, J. Dai, Z. Liu, P. Li and W. Tang, *Phys. Scr.* **96**, 125823 (2021).

[7] H. Zhang, L. Yuan, X. Tang, J. Hu, J. Sun, Y. Zhang, Y. Zhang and R. Jia, *IEEE Trans. Power Electronics* **35** (5), 5157-5179 (2020).

[8] M. H. Wong, A. Takeyama, T. Makino, T. Ohshima, K. Sasaki, A. Kuramata, S. Yamakoshi and M. Higashiwaki, *Appl. Phys. Lett.* **112**, 023503 (2018).

[9] M. Higashiwaki, K. Sasaki, A. Kuramata, T. Masui and S. Yamakoshi, *Phys. Status Solidi A* **211**, 1-240 (2014).

[10] T. Kimoto, *Jpn. J. Appl. Phys* **54**, 040103 (2015).

[11] W. Li, Z. Hu, K. Nomoto, Z. Zhang, J.-Y. Hsu, Q. T. Thieu, K. Sasaki, A. Kuramata, D. Jena and H. G. Xing, *Appl. Phys. Lett.* **113**, 202101 (2018).

[12] H. Zhou, Q. Yan, J. Zhang, Y. Lv, Z. Liu, Y. Zhang, K. Dang, P. Dong and Z. Feng, Q. Feng, J. Ning, C. Zhang, P. Ma, Y. Hao, *IEEE Electron device letters* **40** (11), 1788-1791 (2019).

[13] C. Wang, S. Li, W. Fan, Y. Zhang, X. Zhang, R. Guo, H. Lin, S. Lien and W. Zhu, *Ceramics International* **47**, 29748-29757 (2021).

[14] Y. Oshima, E. Ahmadi, S. Kaun, F. Wu and J. S. Speck, *Semicond. Sci. Technol.* 33, 015013 (2017).

[15] H. Hu, C. Wu, N. Zhao, Z. Zhu, P. Li, S. Wang, W. Tang and D. Guo, *Phys. Status Solidi A* **218**, 2100076 (2021).

[16] Y. Xing, Y. Zhang, J. Han, X. Cao, B. Cui, H. Ma and B. Zhang, *Nanotechnology* **32**, 095301 (2021).

[17] S. Rafique, L. Han and H. Zhao, *Phys. Status Solidi A* **213** (4), 1002-1009 (2016).

[18] H. Murakami, K. Nomura, K. Goto, K. Sasaki, K. Kawara, Q. T. Thieu, R. Togashi, Y. Kumagai, M. Higashiwaki, A. Kuramata, S. Yamakoshi, B. Monemar and A. Koukitu, *Appl. Phys. Express* **8**, 015503 (2015).

[19] Y. Li, X. Xiu, W. Xu, L. Zhang, Z. Xie, T. Tao, P. Chen, B. Liu, R. Zhang and Y. Zheng, *J. Phys. D: Appl. Phys.* **54**, 014003 (2021).

[20]M. Higashiwaki, K. Konishi, K. Sasaki, K. Goto, K. Nomura, Q. T. Thieu, R. Togashi, H. Murakami, Y. Kumagai, B. Monemar, A. Koukitu, A. Kuramata and S. Yamakoshi, *Appl. Phys. Lett.* **108**, 133503 (2016).

[21] V. I. Nikolaev, A. I. Pechnikov, S. I. Stepanov, I. P. Nikitina, A. N. Smirnov, A. V. Chikiryaka, S. S. Sharofidinov, V. E. Bougrov and A. E. Romanov, *Materials Science in Semiconductor Processing* **47**, 16-19 (2016).

[22] F. Alema, B. Hertog, A. Osinsky, P. Mukhopadhyay, M. Toporkov and W. V. Schoenfeld, *J. Cryst. Growth* **475**, 77-82 (2017).

[23] T. I. Shin, H. J. Lee, W. Y. Song, H. Kim, S. W. Kim and D. H. Yoon, *Colloids and Surfaces. A: Physicochem. Eng. Aspects* **313-314**, 52-55 (2008).

[24] X. C. Wu, W. H. Song, W. D. Huang, M. H. Pu, B. Zhao, Y. P. Sun and J. J. Du, *Chem. Phys. Lett.* **328**, 5-9 (2000).

[25] P. Mazzolini, A. Falkenstein, C. Wouters, R. Schewski, T. Markurt, Z. Galazka, M. Martin, M. Albrecht and O. Bierwagen, *APL Mater.* **8**, 011107 (2020).

[26] P. Vogt and O. Bierwagen, *Appl. Phys. Lett.* **108**, 072101 (2016).

[27] X. He, J. Hu, Z. Zhang, W. Liu, K. Song and J. Meng, *Surfaces and Interfaces* **28**, 101585 (2021).

[28] S. Nakagomi and Y. Kokubun, *J. Cryst. Growth* **349**, 12-18 (2012).

[29] S. Ghose, S. Rahman, L. Hong, J. S. Rojas-Ramirez, H. Jin, K. Park, R. Klie and R. Droopad, *J. Appl. Phys.* **122**, 095302 (2017).

[30] D. J. Rogers, A. Courtois, F. H. Teherani, V. E. Sandana, P. Bove, X. Arrateig, L. Damé, P. Maso, M. Meftah, W. El Huni, Y. Sama, H. Bouhnane, S. Gautier, A. Ougazzaden and M. Razeghi, *proc. of SPIE* **11687**, 2D-1 (2021).

[31] S. Nakagomi, S. Kaneko and Y. Kokubun, *Phys. Status Solidi B* **252** (3), 612-620 (2015).

[32] B. Feng, Z. Li, F. Cheng, L. Xu, T. Liu, Z. Huang, F. Li, J. Feng, X. Chen, Y. Wu, G. He and S. Ding, *Phys. Status Solidi A* **218**, 2000457 (2021).